215
5-11-82
($)

(2)

rh. 538

SERI/PR-8143-1-T6
(DE82009398)

# DEVELOPMENT OF COPPER SULFIDE/CADMIUM SULFIDE THIN-FILM SOLAR CELLS

MASTER

Seventh Technical Progress Report, January 13—April 12, 1981

By
J. R. Szedon
W. J. Biter
H. C. Dickey

March 1982

Work Performed Under Contract No. AC02-77CH00178

Westinghouse R&D Center
Pittsburgh, Pennsylvania

**U.S. Department of Energy**

**Solar Energy**

## DISCLAIMER

## DISCLAIMER

"This report was prepared as an account of work sponsored by an agency of the United States Government. Neither the United States Government nor any agency thereof, nor any of their employees, makes any warranty, express or implied, or assumes any legal liability or responsibility for the accuracy, completeness, or usefulness of any information, apparatus, product, or process disclosed, or represents that its use would not infringe privately owned rights. Reference herein to any specific commercial product, process, or service by trade name, trademark, manufacturer, or otherwise, does not necessarily constitute or imply its endorsement, recommendation, or favoring by the United States Government or any agency thereof. The views and opinions of authors expressed herein do not necessarily state or reflect those of the United States Government or any agency thereof."

This report has been reproduced directly from the best available copy.

Available from the National Technical Information Service, U. S. Department of Commerce, Springfield, Virginia 22161.

Price: Printed Copy A04
Microfiche A01

Codes are used for pricing all publications. The code is determined by the number of pages in the publication. Information pertaining to the pricing codes can be found in the current issues of the following publications, which are generally available in most libraries: *Energy Research Abstracts, (ERA); Government Reports Announcements* and Index (*GRA* and I); *Scientific and Technical Abstract Reports (STAR)*; and publication, NTIS-PR-360 available from (NTIS) at the above address.

SERI/PR-8143-1-T6
(DE82009398)
Distribution Category UC-63

# DEVELOPMENT OF COPPER SULFIDE/CADMIUM SULFIDE THIN-FILM SOLAR CELLS

By
J. R. Szedon
W. J. Biter
H. C. Dickey

Seventh Technical Progress Report 13
January 13 to April 12 1981

March 1982

Contract No. XJ-9-8143-1

Westinghouse R & D Center
1310 Beulah Road
Pittsburgh, Pennsylvania 15235

THIS PAGE
WAS INTENTIONALLY
LEFT BLANK

## TABLE OF CONTENTS

# LIST OF ILLUSTRATIONS

# LIST OF TABLES

# ABSTRACT

Unencapsulated thin-film solar cells of the $Cu_2S/CdS$ type have been aged in controlled flowing-gas ambients to characterize changes in their photovoltaic properties. Severe degradation occurring in wet $O_2$ ambients at room temperature probably accounts for the large short-circuit current losses reported earlier. Limited loss (<15% of initial values) in $J_{sc}$ occurs at RT in dry oxygen. No loss can be attributed to moisture in Ar or $N_2$ ambients for exposure times greater than ~2 hrs. Direct measurements of optical absorption in the front $Cu_2S$ layer would be facilitated by an integral $CdS/Cu_2S$ detector on the back surface. Several techniques for making such a detector were successfully demonstrated.

# 1. SUMMARY

The Westinghouse R&D Center is engaged in a program to develop and document cell-processing methods for 9% efficient, low-cost $Cu_2S/CdS$ thin-film solar cells. This is the second quarter of work involving an expansion of the scope of the program. Three tasks are currently being addressed: (1) establishing the reproducibility of a wet-chemistry processing sequence for 9% efficient cells, (2) improving the performance of cells in terms of efficiency and stability, and (3) developing low-cost electrode gridding methods. During the previous two quarters, efforts on the first and third tasks were essentially completed. For the present quarter, emphasis has been placed on the second task. The effort on this task has dealt with two areas: (1) characterizing the dynamic changes in cell performance during aging in several controlled ambients, and (2) exploring methods for producing back-surface $Cu_2S$ layers in cell structures to permit measurement of the light transmitted by the front-surface $Cu_2S$ layer in actual cells.

In our opinion the most important result of the work this quarter is evidence that oxygen and water vapor are required to produce large ($>$ 80% of the initial value) losses in $J_{sc}$ of unencapsulated cells at room temperature. A much smaller loss ($\lesssim$ 20% of the initial current) appears to be associated with oxygen alone. Water vapor in nonoxidizing gases (Ar and $N_2$) had no detectable effect comparable to that for an oxygen carrier case. To our knowledge, earlier reports of degradation in $Cu_2S/CdS$ cells have not involved differentiation of oxygen and water vapor influences.

We have been able to show that short-term ($\lesssim$ 50 hrs) degradation of thin-film $Cu_2S/CdS$ cell performance in dry oxygen is limited and occurs within about 10 hrs at RT. Maximum losses in $J_{sc}$ of 10 to 13%

occur within this period. Over a period of ~200 hrs, the maximum total loss in $J_{sc}$ is from 12 to 15%. The results just cited were obtained for cells which had been previously annealed in hydrogen at 150°C for very long periods (~400 hrs). Cells which had been annealed for only ~150 hrs appeared to have less short-term and total loss in $J_{sc}$ (only about 10% maximum). Aging in dry oxygen at 80°C appears to involve a slightly higher maximum current loss, ~20%. Short-duration anneals were not used, thus we cannot estimate the shortest interval over which most of the loss occurs.

As mentioned above, the most significant losses in $J_{sc}$ and efficiency occur for cells exposed to a moist oxygen ambient. We limited the experiments to room temperature and very high values of relative humidity (75 to 95% RH). The time dependence of $J_{sc}$ for cells aged in this way can be fit by using a sum of two decaying exponential functions. One, having a time constant of 2 to 3.5 hrs, accounts for 18 to 20% loss of the initial $J_{sc}$ value. The other, with a time constant of about 45 hrs, appears to represent 80 to 82% loss of the initial $J_{sc}$ value. Even after 75% loss of their initial $J_{sc}$ capability, cells could be restored to the performance levels recorded before aging by annealing in $H_2$ at 150°C.

Contrary to expectations, there was no significant long-term loss in $J_{sc}$ or other PV parameter when cells were aged in wet argon or wet nitrogen ambients. Losses in $J_{sc}$ were noted after the first 1.5-hr long interval of exposure, suggesting that the hydrogen-annealing step immediately preceding any of the aging intervals may sensitize the $Cu_2S/CdS$ cell and make a 10 to 15% loss in $J_{sc}$ inevitable during any short exposure to a nonreducing atmosphere.

It should be kept in mind that the previous results on cell-aging effects were obtained by using a special stress/evaluation tube in which the cells were mounted, electrically contacted, and retained under controlled gas-ambient conditions for subsequent annealing, measurement, aging, and — in some cases — recovery. We believe that such an approach is necessary if exposure to uncontrolled laboratory ambients and erratic changes in photovoltaic performance of these cells are to be minimized in order that meaningful evaluations can be made.

The mechanism first suggested and most frequently invoked to explain $J_{sc}$ reduction in aged cells is a reduction in optical absorption of the $Cu_2S$ layer due to changes in its stoichiometry as oxidation occurs. To the best of our knowledge, no direct evidence has been presented to confirm that this mechanism actually occurs and accounts for loss of short-circuit current in cells. The topological complexities of the surfaces and heterojunction interfaces in a thin-film cell make it difficult to obtain optical information, by standard methods, which is relevant to cell performance. We feel that relevant information can be obtained by using an integral $CdS/Cu_2S$ detector on the back of a standard cell. In this way, reflection losses with an air interface and errors in positioning are minimized, as compared to using a remote photodetector in conventional measurements.

Several methods of forming $Cu_2S$ layers on the back surfaces of cells were developed during this quarter. In one case, this has been done on completed cells which are laminated to a glass slide. The back surface of the CdS film is exposed by etching or peeling away the copper foil substrate. Photoresponsive detectors on the back surface have been made by wet-CuCℓ processing methods similar to those used for preparing the absorbing front layer in a cell. Although the front and back junctions were isolated under dark evaluation conditions, they were electronically coupled during spectral response measurements.

In order to minimize the possibility of $Cu_2S$ formation along defects or grain boundaries through the full thickness of the CdS film, we attempted to prepare a $Cu_2S$ layer adjacent to the copper foil substrate before the main CdS film was deposited. Our first approach to such a structure was to deposit a thin (1 µm) CdS layer which was then converted to $Cu_2S$ by immersion in CuCℓ solution. Such films did not remain adherent to the copper substrate. We were successful in making an adherent structure and a photoresponsive back-surface detector by evaporating ~ 8000Å of CuCℓ on the copper substrate prior to the standard deposition of CdS. Such a structure would serve for the optical measurement purposes described above. Some problems remain in isolating the contact to the back $Cu_2S$ layer from that to the CdS film for the more complex device structures that would be needed for complete optical measurements.

Future efforts will be directed toward identifying the source of the short-circuit current loss in cells aged in wet oxygen. More comprehensive characterization of the heterojunction behavior will be made to determine if mechanisms controlling diode-opposing current are affected during aging. Measurements will be made to ascertain effects of aging on the optical behavior of $Cu_2S$ layers in cells.

# 2. INTRODUCTION

## 2.1 Objective and Tasks

The objective of this program is to develop and document cell-processing methods for 9% efficient $Cu_2S/CdS$ thin-film solar cells and to assess selected alternate routes for achieving cells with 10% or higher efficiency. Three specific tasks are being addressed for the current phase of the program: (1) improving baseline processing methods to give greater control over the reproducibility of cell performance; (2) investigating means to make more stable, high-efficiency solar cells; and (3) evaluating alternate means of forming the grid electrodes which reduce the high cost of the thick, evaporated gold grids presently being used.

## 2.2 Technical Approach

During this quarter, most of the effort has been directed toward the second task, that of investigating methods to make more stable, high-efficiency solar cells. The status of the other two tasks has been reported previously.(1) Two major lines of study have been followed during this period. One has involved baseline characterizations of state-of-the-art cells aged by storing in controlled, flowing-gas ambients. The second has been exploration of methods for characterizing the optical properties of $Cu_2S$ layers used in thin-film solar cells.

### 2.2.1 Baseline Stability Characterizations

From our own experience and from the literature we appreciate that the performance of $Cu_2S/CdS$ thin-film cells, particularly in terms of short-circuit current, degrades with time during storage or in use. We undertook to characterize, as a function of time, the performance of cells held in controlled atmospheres to understand better the dynamic nature of the degradation effects. For this purpose, a special quartz tube was prepared incorporating the features shown in Figure 1. The stress/evaluation (S/E) tube has a main body of rectangular cross section (2.2 cm × 4.4 cm) which is ~ 30 cm long. The tube is fitted with a flange which is sealed by an O-ring to a plate through which pass an electrical cable and tubes to feed and exhaust the gas for controlling the ambient. The gas inlet tube passes through and supports a copper block on which thin-film cells are mounted, along with a silicon reference cell, as shown in the lower part of Figure 1. Probe contacts to the grid electrodes of each cell are made which are capable of withstanding temperatures of at least 200°C.

Experimental cells are generally selected from those tested earlier and subsequently stored. They are mounted in the S/E tube, which is then sealed and purged with nitrogen. The cells are then given a short (overnight) anneal in pure hydrogen at 150°C to return their performance to near levels achieved before shelf storage. Prior to annealing, hydrogen is flowed through the tube for at least 30 min at room temperature before the tube is inserted into a 150°C furnace. Subsequently, the cells can be evaluated for photovoltaic performance and subjected to controlled conditions of temperature and light under various flowing ambient gases, without being exposed to the atmosphere. In this way, we remove the uncontrolled influences of oxygen and water vapor exposure which are present during conventional testing of cells in a laboratory. Water vapor, in particular, is of concern since the relative humidity of air in our laboratories can range as high as ~ 50%, if only for short periods of time (several hrs to about one day).

Dwg. 7744A32

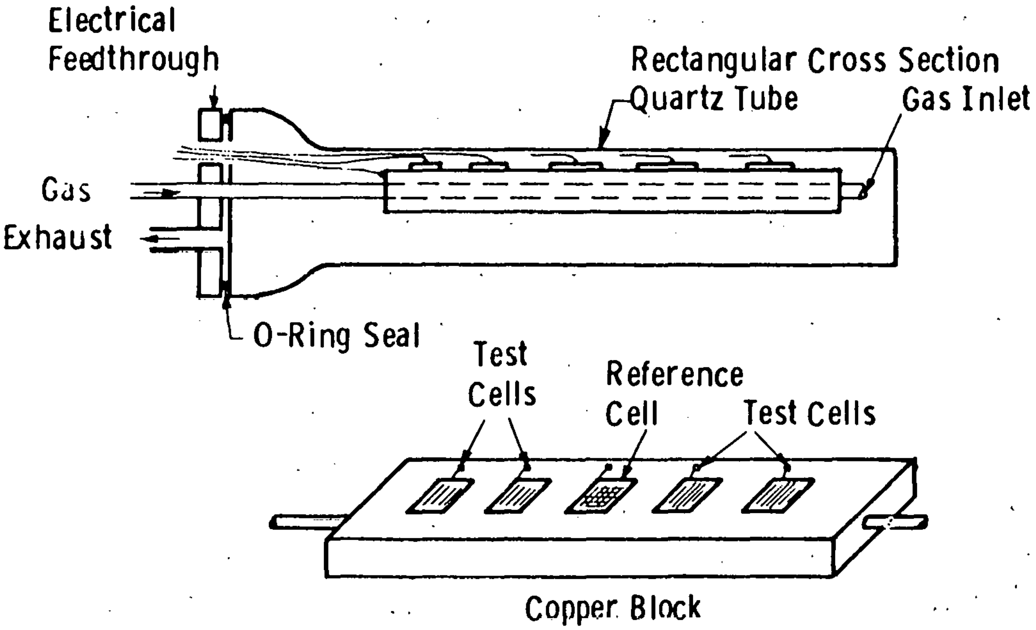

Figure 1. Schematic diagrams showing (top) the stress/evaluation tube for aging and characterizing thin-film cells under controlled ambient conditions and (bottom) the arrangement of test and reference cells.

Initially, we planned to subject cells of moderate performance ($\gtrsim$ 6% conversion efficiency) to aging in pure oxygen, using a series of elevated-temperature conditions not exceeding 100°C. We expected to see measurable short-circuit current degradation within a reasonable period, e.g., about one week. We then planned to humidify the oxygen by passing it through a water bubbler. By using several temperature and humidity conditions, we expected to derive an approximate measure of their effects on the acceleration of cell-performance loss. The method for doing this would be similar in principle to that used by Sbar and Kozakiewicz in considering electrolytic conduction as a failure mechanism in bare- and encapsulated-silicon integrated circuits.(2)

If successful, this initial effort on the characterization of degradation in $Cu_2S$/CdS cells would be combined with studies aimed at pinpointing the physical mechanisms responsible for reduced cell performance. In our opinion a critical area of concern is the ability to characterize more completely the $Cu_2S$ layers used for fabricating cells. An approach to optical characterizations of $Cu_2S$ films in a cell context was the other major task addressed during this quarter.

### 2.2.2 Optical Characterizations of $Cu_2S$ Films in a Cell Configuration

We believe that an important first step in providing basic information on $Cu_2S$ layers in cells is to produce specimens on which optical transmission measurements can be made. We have previously used single-crystal CdS substrates and made simultaneous measurements of local $Cu_2S$ photocurrent, and of light transmission for specimens with a tapered thickness layer of $Cu_2S$. This method allowed estimates to be made of minority-carrier diffusion length, surface recombination velocity, and heterojunction collection efficiency for the devices in question.(3) With single-crystal specimens, this approach is relatively straightforward since the front and back surfaces can be made planar. In addition, the back metal contact need not be in the region of interest optically.

For state-of-the-art thin-film cells of the $Cu_2S$/CdS type, a method must be devised for measuring the amount of light transmitted through the $Cu_2S$ layer. In Ref. 4 we described initial attempts to produce free-standing specimens of CdS films by etching small holes in the copper foil substrate. We planned to use such free-standing areas within actual working cells in order to correlate closely cell performance and $Cu_2S$ optical behavior. Because of the differences in thermomechanical properties of the CdS film and the substrate, the free-standing sections of CdS broke away.

During this period we have explored a variety of methods, other than using free-standing films, for optical characterization of the $Cu_2S$ layers in cells. A common aspect of these efforts has been to apply them in a way to produce a back-surface detector of photons which penetrate the front-surface $Cu_2S$ layer used in a conventional cell. The alternative is to use a remote detector. With a remote detector, internal reflection and light scattering by the small grains and irregularities of the original CdS/Cu interface are expected to preclude accurate and reproducible measurements of $Cu_2S$ spectral transmission which are required for our purposes. An integral detector should avoid these problems. In Section 4 results are presented of our efforts to produce specimens with such detectors.

# 3. BASELINE STABILITY STUDIES OF CELL PERFORMANCE

## 3.1 Light Calibration Using a Silicon Cell as a Reference

In order to perform meaningful in-situ evaluations of cells within the stress/evaluation (S/E) tube, a silicon reference cell is mounted in the center position of the block shown in Figure 1. The simulator-cell distance is adjusted to give the same reading (within several percent) for short-circuit current in the reference cell as was obtained for that cell in open-air testing with 90 mW/cm$^2$ provided by the simulator. Table 1 gives values of percentage differences in photovoltaic parameters for the silicon reference cell and for four thin-film cells after mounting in the S/E tube, compared with values for open-air testing which was done about 15 min earlier. We cannot set the light level to get exactly zero difference for short-circuit current in the silicon reference cell due to slight errors in repositioning the S/E tube with regard to the simulator. In each new set of measurements, the silicon reference-cell data is within several percent of the base values.

For the thin-film cells, the data of Table 1 show a slight enhancement of $J_{sc}$ values as a result of the cells being loaded into the S/E tube. For all other parameters, the percent changes are similar in magnitude to those observed for the reference cell. Until it is noted otherwise, percentage comparisons to be made from this point on will use the cell-parameter values obtained after loading in the S/E tube as the reference standard.

## 3.2 Some Observations on Ambient Influences During Measurement

Table 2 gives a condensed history of photovoltaic parameter behavior for the thin-film cells selected for initial study. All four

Table 1. PERCENT CHANGE IN PV PARAMETERS AFTER MOUNTING CELLS IN (S/E) TUBE

| PV Parameter<br>Cell Designation | $\eta$ | $J_{sc}$ | ff | $V_{oc}$ |
|---|---|---|---|---|
| Si reference | -3.5% | -1.7% | -1.9% | 0.0% |
| 7372X | -2.6% | +2.3 | -4.1% | -0.8% |
| 7382X | -1.7% | +1.4% | -3.0% | 0.0% |
| 7382Y | -1.3% | +1.1% | -2.2% | 0.0% |
| 7382Z | -2.2% | +0.7% | -2.2% | -0.4% |

TABLE 2. HISTORY OF PV PERFORMANCE FOR CELLS SELECTED TO BE AGED IN THE S/E TUBE

CELL NO. 7372X

0.9800CM2

| ANNEAL | VOC | JSC | EFF | F.F | G | R | TIME(HR) | TEMP | COMMENTS |
|---|---|---|---|---|---|---|---|---|---|
| A | 0.496 | 14.95 | 5.96 | 72.3 | 2.20 | 1.35 | 116.0 | 150 | DIP 11-10 |
| B | 0.495 | 15.27 | 5.81 | 70.4 | 2.74 | 1.75 | 208.0 | 150 | |
| C | 0.502 | 17.21 | 6.86 | 71.5 | 1.95 | 1.89 | 159.5 | 150 | |
| D | 0.510 | 15.85 | 6.15 | 68.5 | 3.27 | 2.36 | 320.0 | 21 | STORAGE |
| E | 0.506 | 16.19 | 6.01 | 66.1 | 3.78 | 3.09 | 0.0 | 0 | IN AMPULE ATM. |
| F | 0.499 | 19.59 | 7.16 | 65.9 | 4.51 | 2.59 | 18.5 | 75 | H2 ATM |
| G | 0.499 | 19.05 | 6.89 | 65.2 | 4.62 | 2.81 | 7.0 | 21 | STAG H2 |
| H | 0.503 | 18.98 | 6.85 | 64.6 | 3.65 | 3.57 | 66.0 | 21 | FLOWING H2 |

CELL NO. 7382X

0.8800CM2

| ANNEAL | VOC | JSC | EFF | F.F | G | R | TIME(HR) | TEMP | COMMENTS |
|---|---|---|---|---|---|---|---|---|---|
| A | 0.495 | 15.75 | 6.21 | 71.7 | 1.96 | 1.78 | 116.0 | 150 | DIP 11-10 |
| B | 0.496 | 15.71 | 5.93 | 68.5 | 2.04 | 3.11 | 208.0 | 150 | |
| C | 0.503 | 17.78 | 6.88 | 69.3 | 1.82 | 2.78 | 150.5 | 150 | |
| D | 0.508 | 16.84 | 6.42 | 67.5 | 3.38 | 2.71 | 320.0 | 21 | STORAGE |
| E | 0.508 | 17.10 | 6.29 | 65.1 | 4.09 | 3.32 | 0.0 | 0 | IN AMPULE ATM. |
| F | 0.500 | 20.40 | 7.28 | 64.2 | 5.24 | 2.90 | 16.5 | 75 | H2 ATM. |
| G | 0.504 | 19.12 | 7.04 | 65.8 | 2.90 | 3.44 | 7.0 | 21 | STAG. H2 |
| H | 0.498 | 20.20 | 6.90 | 61.7 | 4.38 | 4.17 | 66.0 | 21 | FLOWING H2 |

CELL NO. 7382Y

0.9600CM2

| ANNEAL | VOC | JSC | EFF | F.F | G | R | TIME(HR) | TEMP | COMMENTS |
|---|---|---|---|---|---|---|---|---|---|
| A | 0.490 | 15.68 | 6.27 | 73.5 | 1.07 | 1.65 | 116.0 | 150 | DIP 11-10 |
| B | 0.495 | 15.86 | 6.31 | 72.3 | 1.75 | 1.69 | 208.0 | 150 | |
| C | 0.503 | 17.70 | 7.03 | 71.1 | 1.93 | 2.05 | 159.5 | 150 | |
| C′ | 0.506 | 17.50 | 6.61 | 67.2 | 0.76 | 4.11 | 322.0 | 150 | |
| D | 0.507 | 17.50 | 6.22 | 63.1 | 2.35 | 4.98 | 0.0 | 0 | STORAGE |
| E | 0.507 | 17.71 | 6.15 | 61.7 | 4.50 | 4.57 | 0.0 | 0 | IN AMPULE ATM. |
| F | 0.500 | 20.69 | 7.10 | 61.7 | 1.38 | 4.93 | 16.5 | 75 | H2 ATM. |
| G | 0.501 | 17.99 | 6.28 | 62.8 | 0.92 | 5.40 | 7.0 | 21 | STAG. H2 |
| H | 0.504 | 20.49 | 6.75 | 58.8 | 2.85 | 5.62 | 66.0 | 21 | FLOWING H2 |

CELL NO. 7382Z

0.9700CM2

| ANNEAL | VOC | JSC | EFF | F.F | G | R | TIME(HR) | TEMP | COMMENTS |
|---|---|---|---|---|---|---|---|---|---|
| A | 0.491 | 14.90 | 5.93 | 73.0 | 1.82 | 1.30 | 116.0 | 150 | DIP 11-10 |
| B | 0.496 | 14.89 | 5.93 | 72.3 | 1.26 | 2.13 | 208.0 | 150 | |
| C | 0.504 | 17.38 | 6.85 | 70.3 | 1.89 | 2.38 | 159.5 | 150 | |
| D | 0.511 | 16.29 | 6.24 | 67.5 | 2.08 | 3.64 | 320.0 | 21 | STORAGE |
| E | 0.509 | 16.43 | 6.11 | 65.8 | 2.63 | 3.98 | 0.0 | 0 | IN AMPULE ATM. |
| F | 0.504 | 18.35 | 7.15 | 69.6 | 1.72 | 2.68 | 16.5 | 75 | H2 ATM. |
| G | 0.500 | 14.85 | 5.85 | 71.0 | 1.05 | 2.89 | 7.0 | 21 | STAG. H2 |
| H | 0.506 | 19.73 | 7.18 | 64.7 | 3.29 | 3.61 | 66.0 | 21 | FLOWING H2 |

cells (three of which used the same lot of CdS) were originally processed together with regard to $Cu_2S$ layer formation, electrode gridding, and preliminary tests. They were given long periods of initial annealing in $H_2$ at 150°C. After 484 hrs (Anneals A through C), three of the cells were put into storage in a cabinet under a slight positive pressure of house nitrogen. The fourth cell (#7382Y), which had the highest efficiency of the group, was annealed for another 322 hrs in $H_2$ at 150°C. At this point, after anneal C', its efficiency had dropped slightly, primarily due to a change in the fill-factor value.

The four cells were then retested, giving the results for Anneal D in Table 2. All three of the cells which were stored under a slight positive pressure of nitrogen exhibited reduced performance. As shown in Table 3, conversion efficiency for these cells was down from 6 to 10% as a result of the storage. Approximately two thirds of the percentage change in efficiency is associated with reductions in short-circuit current.

We have already commented in Section 3.1 on the slight changes in measured photovoltaic parameters which resulted when the cells were installed within the stress/evaluation tube. Those changes (given in Table 1 and involving comparisons of results for Anneals D and E in Table 2) were much smaller than the changes that were noted after storing the three cells in question for two weeks.

Further sensitivity of cell performance to a controlled atmosphere within the stress/evaluation tube is evident from the data for conditions designated as Anneals F, G, and H in Table 2. Overnight treatment in flowing hydrogen at a moderate temperature of 75°C (Anneal F) yielded higher cell performance than did any previous anneal. Efficiency values increased by 15 to 20% and, as in the case of the storage conditions, short-circuit current increases were the controlling parameter. After being stored in the S/E tube at RT under stagnant hydrogen for seven hrs (Anneal G), the cells suffered decreases in short-circuit current and efficiency ranging from 3 to about 19%. As a

TABLE 3. PERCENTAGE CHANGES IN PV PERFORMANCE FOR THIN-FILM CELLS DURING STORAGE FOR 322 HOURS IN NITROGEN DRY BOX

| PV Parameter<br>Cell No. | $\eta$ | $J_{sc}$ | ff | $V_{oc}$ | $(ffV_{oc})$ |
|---|---|---|---|---|---|
| 7372X | -10.3% | -7.9% | -4.2% | +1.6% | -2.6% |
| 7382X | - 6.4% | -5.2% | -2.6% | +1.0% | -1.1% |
| 7382Z | - 8.9% | -6.3% | -4.0% | +1.4% | -3.1% |

result of storage in the S/E tube over one weekend at RT under flowing $H_2$ (Anneal H), the cells exhibited considerable scatter in the percentage change in efficiency (from -2 to +23%) and in short-circuit current density (from -1 to +33%).

The results of initial tests on cells in the S/E tube established that significant differences in cell performance resulted from each of several ambient conditions (flowing $H_2$ at 75°C and at 21°C and stagnant $H_2$ at 21°C). These results have two important ramifications. First, they demonstrate that the S/E tube, under flowing-gas conditions, is an effective method for controlling the gas ambient in which $Cu_2S/CdS$ cells are aged and evaluated. Secondly, the increases in short-circuit current due to very mild reducing ambients of flowing hydrogen and the loss of current merely due to cell exposure to a stagnant hydrogen ambient suggest that the photocurrent in these cases is modulated by a very sensitive surface mechanism. It seems unlikely that the stoichiometry of the $Cu_2S$ layer could be affected by the conditions we used in these studies. Furthermore, if that were the case one would expect more significant changes in junction-opposing current as reflected in the open-cirucit voltage. There is no evidence for such changes in the data of Table 2.

## 3.3 Performance of Cells Aged in Dry Oxygen

### 3.3.1 Dry Oxygen at Room Temperature

The four cells used for the initial studies of ambient effects during measurement, as discussed in Section 3.2, were given new identification numbers for an experiment involving aging within the stress/evaluation (S/E) tube in an ambient of dry oxygen.* Table 4 gives initial values of $V_{oc}$, $J_{sc}$, and fill factor for the cells together

---

*Matheson Super Pure Oxygen with less than 100 ppm of water was used.

TABLE 4. SUMMARY OF CHANGES IN PHOTOVOLTAIC PERFORMANCE FOR CELLS AGED AT ROOM TEMPERATURE (~ 21°C) IN DRY OXYGEN

| | Cell Number | | | |
|---|---|---|---|---|
| | 10000<br>(7372X)* | 20000<br>(7382X) | 30000<br>(7382Y) | 40000<br>(7382Z) |
| A. Initial $J_{sc}$ (mA/cm$^2$) | 18.980 | 20.200 | 20.490 | 19.730 |
| $\eta$ (%) | 6.850 | 6.900 | 6.750 | 7.180 |
| $V_{oc}$ (volt) | 0.503 | 0.498 | 0.504 | 0.506 |
| ff | 0.646 | 0.617 | 0.588 | 0.647 |
| B. Percentage changes after first 1.5 hrs of aging | | | | |
| $J_{sc}$ | -7.5% | -8.7% | -9.2% | -8.7% |
| $\eta$ | -1.8% | +0.4% | -5.5% | -4.7% |
| $V_{oc}$ | +1.0% | +2.4% | +1.2% | +0.2% |
| ff | +5.1% | +7.8% | +2.9% | +4.3% |
| C. Percentage changes after 219 hrs of aging | | | | |
| $J_{sc}$ | -12.2% | -13.0% | -14.9% | -13.9% |
| $\eta$ | -9.1% | -7.0% | -19.7% | -12.5% |
| $V_{oc}$ | +1.6% | +3.0% | +1.8% | +0.8% |
| ff | +1.9% | +4.2% | -7.1% | +0.9% |

*Former designation in Table 2.

with percentage changes after the first aging interval (1.5 hrs) and after 217 hrs of aging in dry oxygen.

Of all the photovoltaic performance parameters, short-circuit current exhibited the most consistent percentage changes: 8 to 9 percent reductions after the first 1.5 hrs, 10 to 13 percent after the first 4.5 hrs, and 12 to 15% reductions over the course of 219 hrs. Percentage changes in fill-factor values covered wider ranges: +3 to +8% for the first 1.5-hr period and +4 to -7% for the 219-hr period. Open-circuit voltage exhibited small increases (<2%) initially and (<3%) over the course of the entire aging period. As a result of the wide ranges in fill-factor changes, the percentage changes in efficiency were affected. These changes ranged from +0.4% to -5.5% for the initial 1.5-hr period and from -7.0% to -19.7% for the 219-hr period.

A second group of cells was similarly installed in the S/E tube at a later date and aged in dry oxygen at room temperature. Results for those cells are given in Table 5. They are similar to those in Table 4 except for two features: (1) the percentage changes in fill-factor values were less than for the first group of cells and (2) the changes in short-circuit current after the first 1.5 hrs of aging were much less than for the first group of cells.

The cells of the second group differed from those in the first group in terms of their annealing history prior to installation in the S/E tube. They had been annealed for only 144 hrs in hydrogen at ~ 150°C, whereas those in the first group had been annealed for at least 482 hrs. Cell #30000 of the first group had been annealed in hydrogen for a total of 805 hrs. (We speculate that the long anneal may be associated with the fill-factor reduction for long-term aging, which was counter to the trend in the first group of cells.) In addition to shorter annealing for cells in the second group, two of them (#11001 and #11002) were fabricated with electroplated rather than evaporated grids. Because of the process requirements for electroplating, these cells had an $SiO_2$ film covering the $Cu_2S$ surface.* Figure 2 gives

---

*Processing details and performance of cells with electroplated grids are discussed on pp. 27-36 of Ref. 1.

TABLE 5. SUMMARY OF CHANGES IN PV PERFORMANCE FOR A SECOND GROUP OF CELLS AGED AT RT IN DRY OXYGEN

| | Cell Numbers (Original Designations in Parentheses) | | | |
|---|---|---|---|---|
| | 11001 | 11002 | 11003 | 11004 |
| | (7143B) | (7083A) | (7432X) | (7432Y) |
| Initial $J_{sc}$ (mA/cm$^2$) | 17.400 | 18.730 | 19.050 | 18.480 |
| $\eta$ (%) | 6.880 | 6.690 | 6.600 | 6.730 |
| $V_{oc}$ (volt) | 0.483 | 0.475 | 0.491 | 0.495 |
| ff | 0.737 | 0.677 | 0.641 | 0.662 |
| Percentage changes after first 1.5 hrs of aging | | | | |
| $J_{sc}$ | -6.2% | -6.0% | -10.7% | -8.6% |
| $\eta$ | -5.2% | -4.2% | -6.5% | -7.6% |
| $V_{oc}$ | +0.8% | +1.7% | +1.6% | +0.4% |
| ff | +0.1% | +0.3% | +3.0% | +0.8% |
| Percentage changes after 260 hrs of aging | | | | |
| $J_{sc}$ | -5.3% | -1.1% | -10.7% | -10.1% |
| $\eta$ | -5.1% | +0.6% | -8.0% | -10.3% |
| $V_{oc}$ | +1.7% | +2.5% | +2.4% | +1.0% |
| ff | -1.4% | -0.7% | +0.5% | -1.1% |

Curve 730524-B

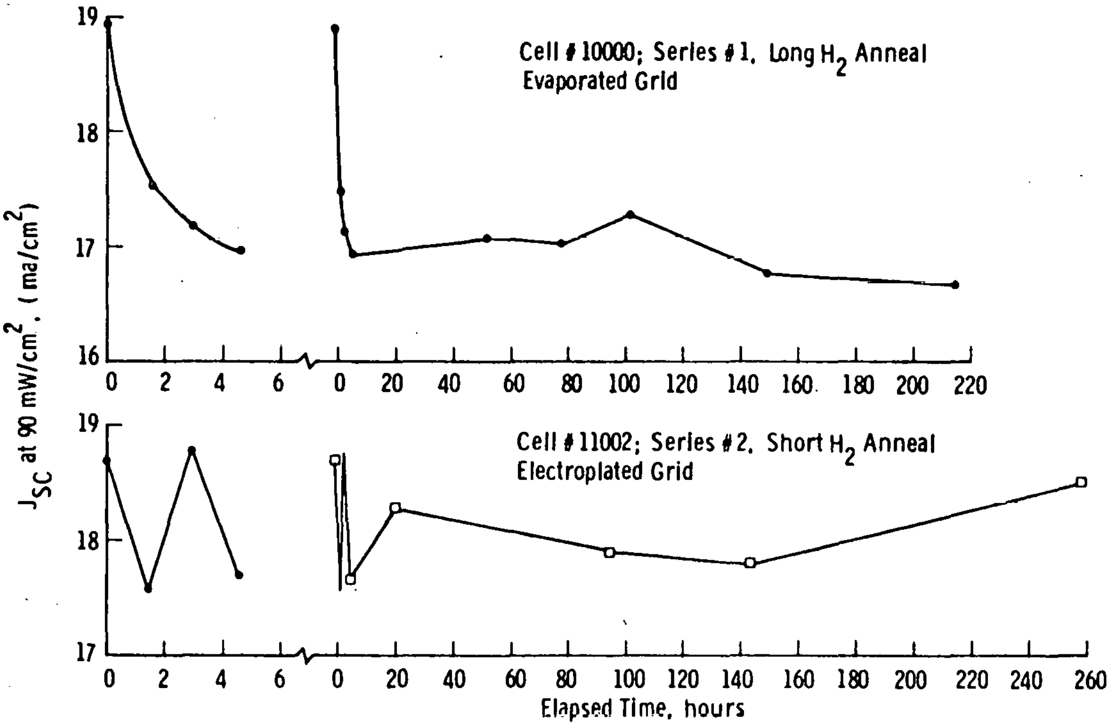

Figure 2. Examples of short-circuit current density changes during short- and long-term aging in dry oxygen for two of the eight cells treated in the text.

typical behavior of the short-circuit current changes for cells (one with an electroplated grid) from the two groups which were studied.

From these experiments we conclude that standard cells aged in pure $O_2$ at room temperature exhibit a measurable loss (from 8 to 11%) in short-circuit current during the first 1.5-hr period. (Two cells with electroplated grids exhibited a somewhat smaller loss of about 6%.) Over a long period (219 hrs), additional losses of 4 to 6% in short-circuit current were observed in cells which had been annealed extensively (~ 500 to 800 hrs) in $H_2$ prior to these experiments. About half of that additional loss occurred during the first 4.5 hrs of aging. Cells which had been annealed for about 144 hrs exhibited at most another 1.5% loss in short-circuit current during additional aging between 1.5 and 260 hrs. (Only two cells were used for this experiment, thus the results must be taken with some caution.) For cells with electroplated grids and an SiO film over the $Cu_2S$ layer, subsequent aging appeared to result in some recovery of the current. For long-term aging, the total observed percentage loss in short-circuit current for these cells was less than half that for the standard cells.

### 3.3.2 Dry Oxygen at 80°C

The second group of cells discussed in Section 3.3.1, which were aged in dry oxygen at room temperature, were then annealed in situ for 24.5 hrs in hydrogen at 150°. This resulted in photovoltaic parameters being restored to or slightly above those values measured prior to room temperature aging. The cells were then aged at 80°C (achieved by placing the S/E tube in a tubular furnace). They were removed from the furnace twice (after 80 and after 160 hrs had elapsed), cooled and measured in situ.

Results of changes in performance are given in Table 6. For the cells with evaporated grids, large reductions in $J_{sc}$ (~ 20%) and in $\eta$ (~ 23%) were observed after 80 hrs, with some very slight recovery occurring after 160 hrs. For the cells with evaporated grids, there

TABLE 6. CHANGES IN PV PERFORMANCE FOR CELLS AGED AT 80°C IN DRY OXYGEN

| | Cell Number | | | |
|---|---|---|---|---|
| | 11001 | 11002 | 11003 | 11004 |
| A. Initial $J_{sc}$ (mA/cm$^2$) | 18.070 | 19.000 | 19.290 | 19.240 |
| $\eta$ (%) | 7.040 | 6.830 | 6.850 | 6.770 |
| $V_{oc}$ (volt) | 0.481 | 0.474 | 0.492 | 0.491 |
| ff | 0.729 | 0.670 | 0.650 | 0.645 |
| B. Percentage changes after 80 hrs of aging | | | | |
| $J_{sc}$ | -6.6% | -2.8% | -20.1% | -20.4% |
| $\eta$ | -9.9% | -4.7% | -23.1% | -21.7% |
| $V_{oc}$ | -1.0% | -0.2% | -0.8% | -0.6% |
| ff | -2.5% | -1.6% | -3.1% | -1.1% |
| C. Percentage changes after 160 hrs of aging | | | | |
| $J_{sc}$ | -8.9% | -7.0% | -17.6% | -19.1% |
| $\eta$ | -9.8% | -4.7% | -18.1% | -20.2% |
| $V_{oc}$ | +1.2% | +2.9% | +1.6% | +1.8% |
| ff | -2.3% | -0.3% | -2.3% | -3.3% |

were short-circuit current reductions of 3 to 7% after 80 hrs and 7 to 9% after 100 hrs. Reductions in efficiency values were only 5% to 10%, being held constant by some improvement in $V_{oc}$ over the course of 160 hrs of aging.

Our intent was to age the cells longer at 80°C, but a furnace-controller failure resulted in the cells being returned to room temperature during an overnight interval. As a result of this low-temperature condition, the cells regained at least half of the short-circuit current lost during the first 160 hrs at 80°C, as shown in Section A of Table 7. (One of the electroplated cells recovered nearly all of the current lost.) Open-circuit voltage values for all cells and fill values for the cells with plated grids were not strongly affected by the furnace failure. Fill-factor values for the cells with evaporated grid cells were slightly worse.

Aging in dry $O_2$ at 80°C was resumed and the cells were measured after additional intervals of 80, 160, and 240 hrs. Results of these measurements are given in Sections B, C, and D of Table 7. They show that for all cells the percentage losses in $J_{sc}$ over 240 hrs of aging were comparable to or slightly less than the losses measured over a period of 160 hrs in the initial aging tests at 80°C.

We feel it is safe to conclude that maximum percentage losses in $J_{sc}$ should not exceed 20% for cells with evaporated grids aging in dry oxygen at 80°C for periods of as long as 160 to 400 hrs. For cells with plated grids, the maximum losses in $J_{sc}$ for comparable times would probably be lower, ~ 10 to 15%.

## 3.4 Degradation of Cells Aged in Wet Oxygen at Room Temperature

Effects of aging cells in flowing wet oxygen at room temperature were studied by using the first group of cells (Table 4) initially aged in a dry $O_2$ ambient at room temperature. After those studies, the cells were annealed in the S/E tube at 150°C in flowing hydrogen for a period of 41 hrs. As a result of this conditioning, the performance of the

TABLE 7. PERCENTAGE CHANGES IN PV PERFORMANCE OF CELLS DURING A SECOND SERIES OF AGING TESTS AT 80°C IN DRY OXYGEN (ALL REFERENCED TO DATA IN SECTION A, TABLE 6).

| | Cell Number | | | |
|---|---|---|---|---|
| | 11001 | 11002 | 11003 | 11004 |
| A. Change after furnace failure | | | | |
| $J_{sc}$ | -4.4% | -1.1% | -8.7% | -11.0% |
| $\eta$ | -5.5% | +0.1% | -13.0% | -16.5% |
| $V_{oc}$ | +1.7% | +2.5% | +1.4% | +1.6% |
| ff | -2.7% | +0.6% | -6.2% | -7.9% |
| B. Change after 80 hrs, 80°C | | | | |
| $J_{sc}$ | -6.6% | -3.8% | -15.1% | -16.7% |
| $\eta$ | -8.7% | -3.2% | -20.3% | -22.5% |
| $V_{oc}$ | +0.8% | +1.7% | +0.8% | +0.8% |
| ff | -3.0% | +0.7% | -6.9% | -7.6% |
| C. Change after 160 hrs, 80°C | | | | |
| $J_{sc}$ | -7.0% | -4.2% | -15.1% | -16.1% |
| $\eta$ | -9.5% | -2.9% | -24.1% | -26.1% |
| $V_{oc}$ | +0.4% | +1.9% | +0.8% | +0.8% |
| ff | -3.2% | +1.2% | -11.2% | -12.6% |
| D. Change after 240 hrs, 80°C | | | | |
| $J_{sc}$ | -10.3% | -6.3% | -14.2% | -19.4% |
| $\eta$ | -13.6% | -6.9% | -19.0% | -27.8% |
| $V_{oc}$ | 0.0% | +1.3% | +0.8% | +0.8% |
| ff | -3.7% | 0.0% | -1.1% | -11.0% |

cells was restored very close to the reference values given in Section A of Table 4. The largest percentage deviations from the reference values were -1.8%, -3.6%, -1.4%, and +4.3% for $J_{sc}$, $\eta$, $V_{oc}$, and fill-factor values, respectively.

Immediately after these measurements, a flowing-gas ambient of wet $O_2$ at room temperature was established for these cells in the S/E tube. Dry oxygen was bubbled through room temperature distilled water and fed into the S/E tube. Gas from the S/E tube was fed into a plastic box containing an Abbeon brand hygrometer. Tubing of 0.64 cm (0.25 in) diameter was used for all the gas connections. During an initial series of tests, the hygrometer indicated relative humidity values of 75 to 80%. For later tests involving aging for more than 4.5 hrs, indicated values of relative humidity were in the range of 85 to 95%. We did not consider it worthwhile to expend greater effort for a tighter control of humidity in these experiments.

After our experiences with cells aged in dry oxygen, we found the results of aging in wet oxygen to be different in several respects. First, the data was less erratic. There was also less difference between the performance of individual cells. Finally, the changes in cell performance were much larger than for the case of aging in dry oxygen.

Figure 3 shows $J_{sc}$ data for the four cells in question, which were aged for a total elapsed time of ~45 hrs in wet oxygen. We observe that the data points for these cells can be fit reasonably well by a function with double exponential decay. The solid curve in Figure 3 is the sum of two exponentials, one having a normalized amplitude of 0.18 and a time constant of 3.5 hrs, the other having an amplitude of 0.82 and a time constant of 46.5 hrs. Detailed fitting of the curves for each of the four cells can be done (without adjusting the component amplitudes) by choosing the shorter time constants to lie between 2 and 3.5 hrs, the longer ones between 44 and 46.5 hrs. We note in passing that the four cells in question were initially exposed to wet $O_2$ for two

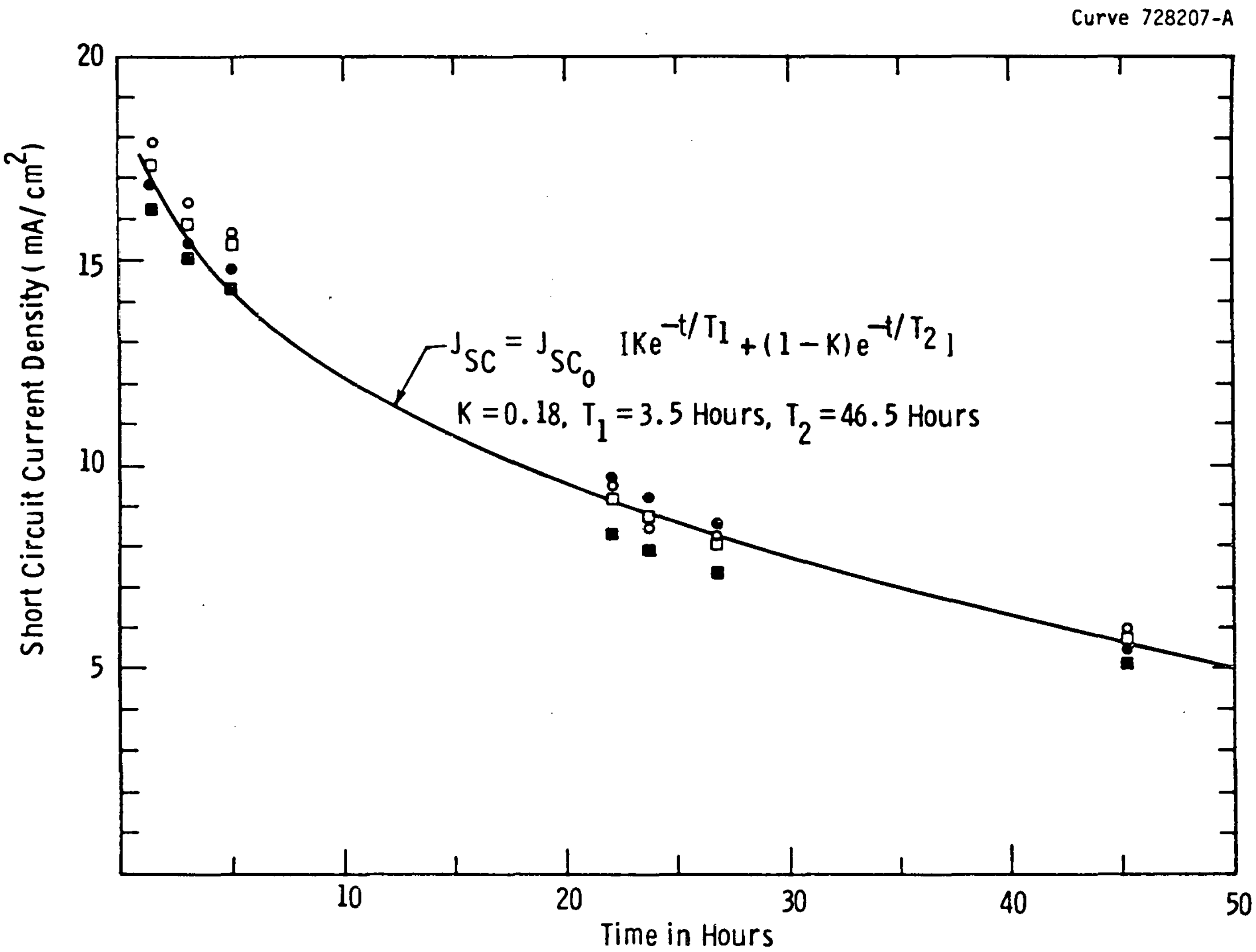

Figure 3. Short-circuit current degradation in four cells aged in wet oxygen at RT.

1.5-hr intervals, then annealed in $H_2$ at 150°C for 139 hrs before being given the exposures used to produce Figure 3. For those initial short exposures, the rate of loss of $J_{sc}$ was somewhat greater than that shown in Figure 3. Using the double exponential fit with the same component amplitudes, we estimate a value for the short time constant of about 1 hr for the initial exposure results. This may indicate that the value of the short time constant is dependent on the previous history of exposure to wet $O_2$ or of annealing in hydrogen.

Figure 4 shows short-circuit current behavior for the four cells in question, beginning with the initial 3-hr exposure in wet $O_2$ at the left through the second and longer exposure to wet $O_2$ (terminating at about 225 hrs on the time scale used). The main purpose of this figure is to present the results for subsequent changes in $J_{sc}$ during annealing in $H_2$ at 150°C (shown for $t > 225$ hrs). Figure 6 is a companion figure to demonstrate that the effects of degradation and recovery of $J_{sc}$ control the efficiency behavior of the cell. In Figure 7, similar treatment of the fill-factor data shows that exposure to wet $O_2$ had relatively little effect on fill-factor values of the cells.

### 3.5 Aging in Wet Argon and Nitrogen

A new group of four cells was selected for aging studies in wet atmospheres of nonreactive gases. In this way we expected to be able to separate the relative influences of oxygen and moisture which were involved in the wet $O_2$ aging studies of the previous section.

The first series of tests was done for cells aged in flowing argon of relative humidity values from 73 to ~100%. Several aging intervals of overnight and one weekend were used, but most intervals were of a 1.5-hr duration. Three cells exhibited ~ 5% reductions in $J_{sc}$ (with regard to the starting value as references) during the first 1.5-hr interval. (One cell exhibited no loss on that occasion.) One cell was 9% lower than the reference value of $J_{sc}$ after one weekend-anneal interval. This was the largest deviation in $J_{sc}$ over the course of the

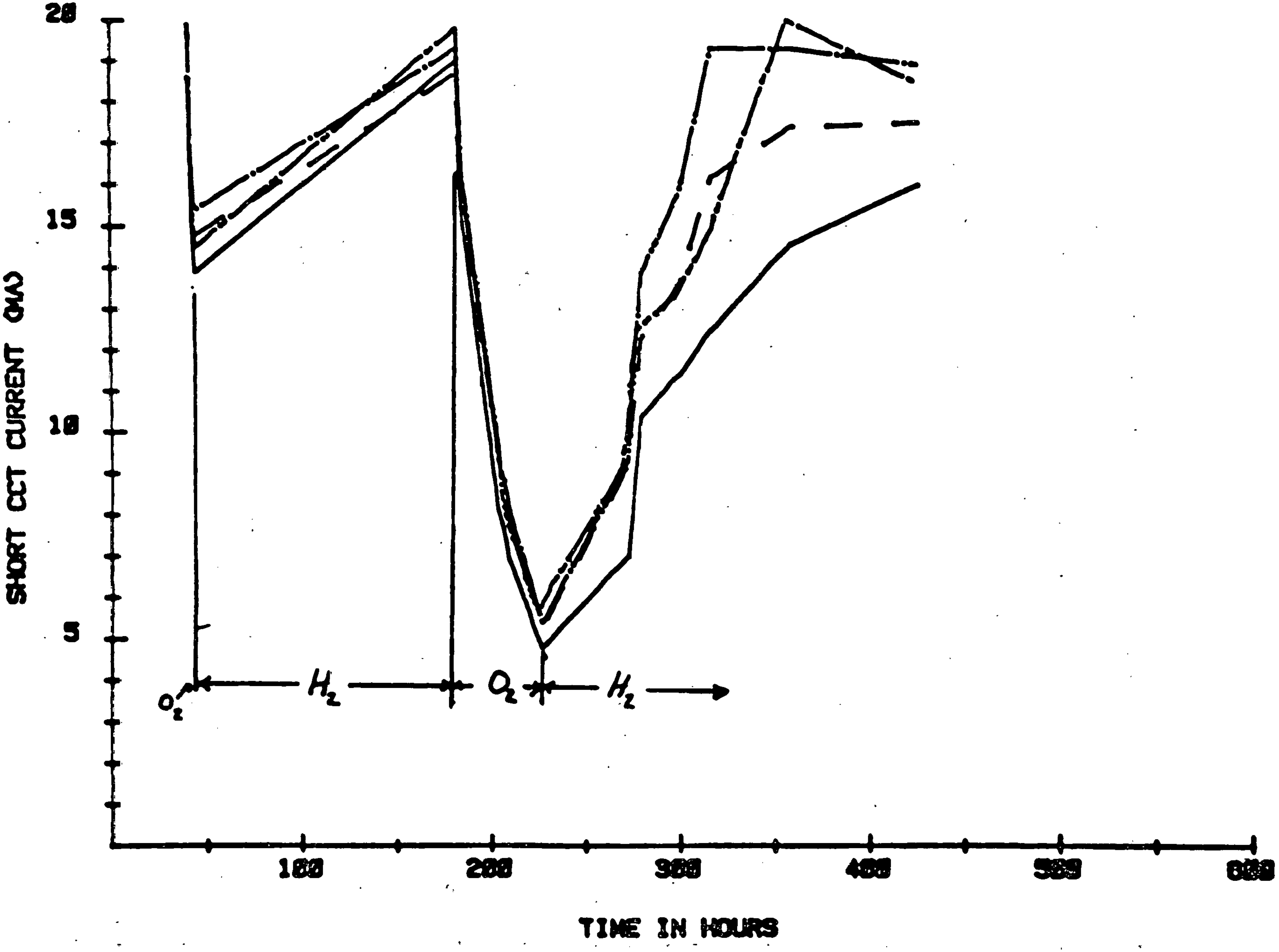

Figure 4. History of $J_{sc}$ changes during aging at RT in wet oxygen and annealing in hydrogen at 150°C.

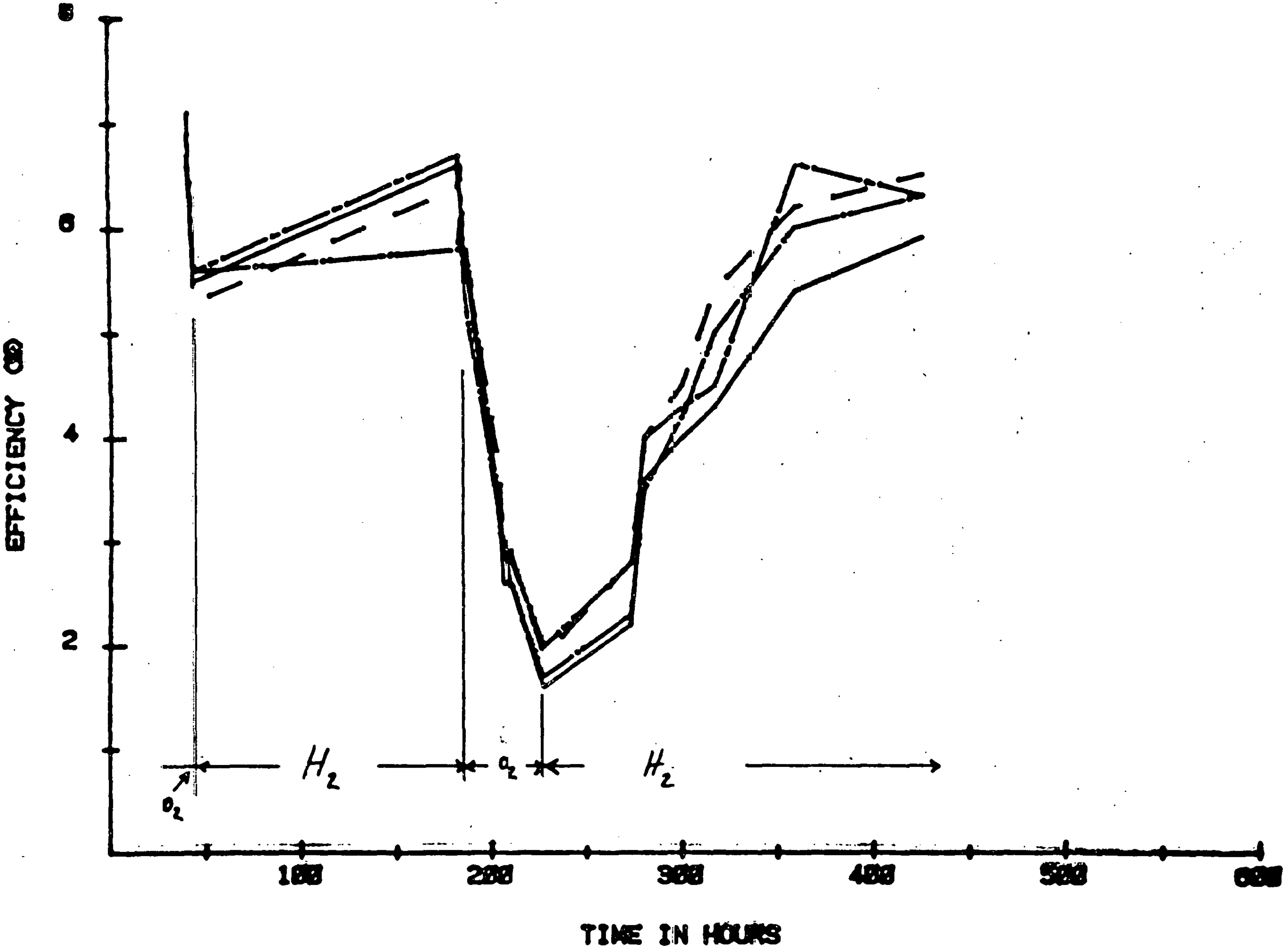

Figure 5. History of efficiency degradation in wet oxygen and recovery during hydrogen annealing.

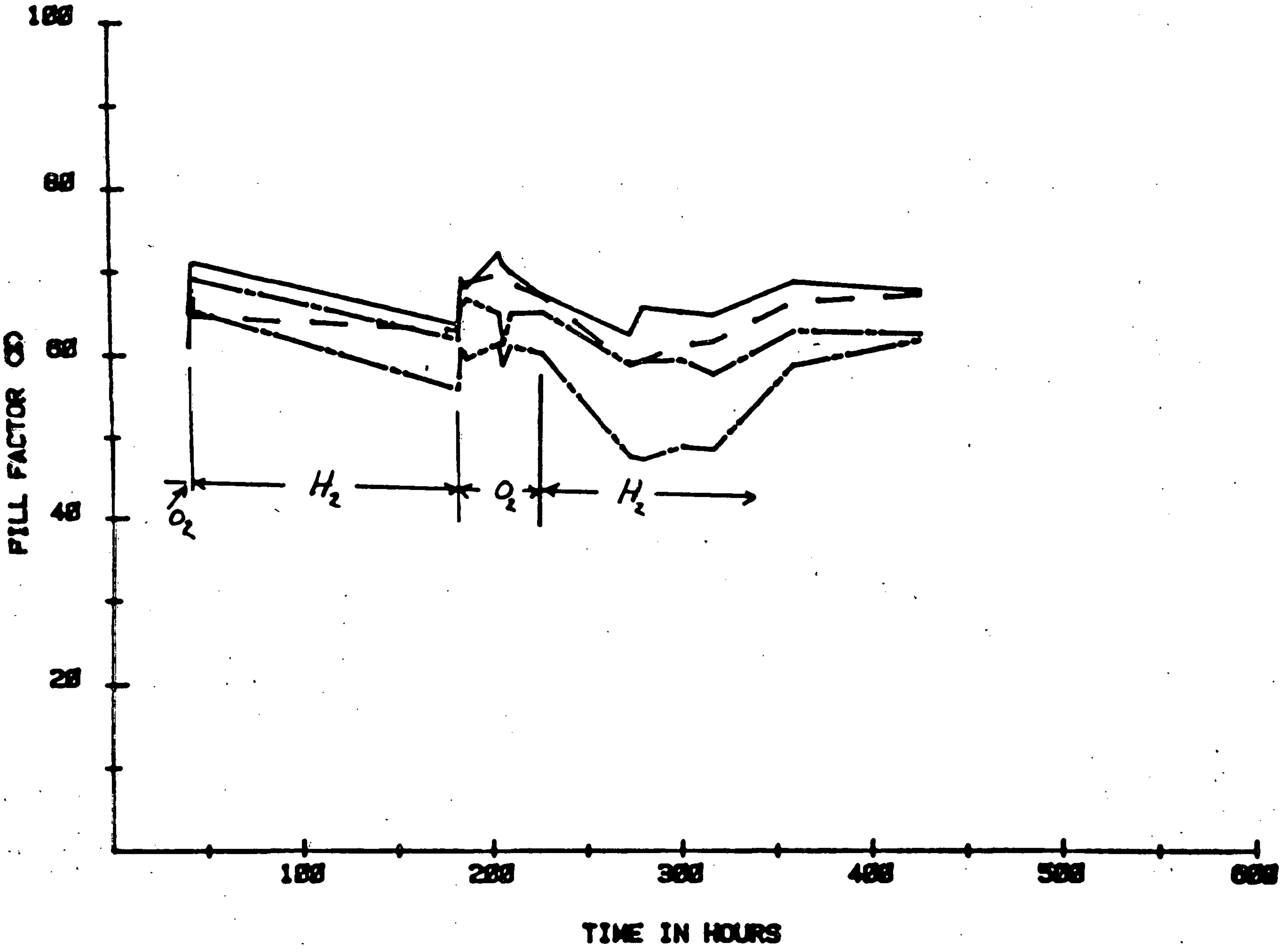

Figure 6. Fill-factor behavior in wet oxygen and during hydrogen annealing.

115-hr total time in wet Ar, and it occurred between two intervals giving $J_{sc}$ values equal to or larger than the reference value for the cell in question. In other words, no consistent trends were noted for changes in $J_{sc}$ in the cells subjected to room temperature aging in wet argon. Section A of Table 8 gives the total aging history (Anneals C through M) for a typical cell in the group. Note that the last row of data for Anneal N shows a 17% loss in $J_{sc}$ resulting from a 1.5-hr exposure to wet $O_2$ in line with the observations discussed in Section 3.4.

After the short exposure to wet $O_2$, the cells were given a 20-hr anneal in $H_2$ at 150°C to verify that they were responsive to appropriate atmospheric conditions. Values of $J_{sc}$ after this anneal ranged from 4% higher to 5% lower than for the reference values prior to wet argon exposure. The new values of $J_{sc}$ were used subsequently as references for changes during the course of aging in wet $N_2$ at RT over a total time of ~ 300 hrs. After the first 1.5 hrs of aging, $J_{sc}$ values dropped by 7 to 10%. Additional aging did not reveal any clear trends. As in the case of wet Ar aging, performance changes were erratic. For three of the cells, $J_{sc}$ values did not drop any lower and reached or exceeded the new reference values at some time during subsequent aging. The fourth cell exhibited somewhat larger changes in $J_{sc}$ but without any clear trend to suggest consistently greater degradation with time. Section B of Table 8 gives the complete aging history in wet $N_2$ of the same cell treated in Section A. (The cell numbers differ only for convenience in logging the data by computer.)

In reviewing the overall effect of wet Ar or wet $N_2$ ambients on cell performance, we find no consistent long-term trends suggesting degradation. Values of $J_{sc}$ did change erratically during these studies, as was observed for long-term aging in dry $O_2$ at RT and at 80°C. In light of these observed fluctuations during long-term aging, it is interesting that all cells exhibit a decrease in $J_{sc}$ during the first short interval of aging in wet Ar or $N_2$. The same was true of cells aged in dry $O_2$. This suggests that the high-temperature hydrogen-

TABLE 8. TYPICAL EXAMPLES OF CELL PERFORMANCE DURING THE COURSE OF AGING IN FLOWING WET ARGON AND NITROGEN ATMOSPHERE

A. Argon

CELL NO. 13001

1.1100CM2

| ANNEAL | VOC | JSC | EFF | F.F | G | R | TIME(HR) | TEMP | COMMENTS |
|---|---|---|---|---|---|---|---|---|---|
| A | 0.492 | 15.98 | 5.70 | 65.2 | 3.71 | 3.39 | 0.0 | 21 | STORAGE |
| B | 0.488 | 17.48 | 6.28 | 66.3 | 3.98 | 2.65 | 21.0 | 150 | FLOWING H2 |
| C | 0.497 | 16.70 | 6.19 | 67.1 | 4.16 | 2.23 | 1.5 | 21 | FLOW AR 73% HUM. |
| D | 0.499 | 17.30 | 6.41 | 66.8 | 3.22 | 2.99 | 1.5 | 21 | FLOW AR 85% HUM. |
| E | 0.499 | 17.06 | 6.36 | 67.2 | 3.89 | 2.41 | 1.5 | 21 | FLOW AR 89% HUM. |
| F | 0.499 | 17.24 | 6.36 | 66.5 | 2.60 | 3.45 | 0.7 | 21 | FLOW AR @ 97% HUM. |
| G | 0.495 | 17.36 | 6.32 | 66.2 | 4.57 | 2.40 | 16.0 | 21 | FLOW AR @ 100% HUM. |
| H | 0.500 | 17.48 | 6.42 | 66.2 | 2.50 | 3.62 | 1.5 | 21 | FLOW AR @ 99.5% HUM |
| I | 0.497 | 17.54 | 6.42 | 66.3 | 3.94 | 2.74 | 2.5 | 21 | FLOW AR @ 99% HUM. |
| J | 0.489 | 16.94 | 6.11 | 66.4 | 3.52 | 2.88 | 2.5 | 21 | FLOW AR @ 98% HUM. |
| K | 0.499 | 17.24 | 6.36 | 66.6 | 3.23 | 3.08 | 16.0 | 21 | FLOW AR @ 99% HUM. |
| L | 0.494 | 16.82 | 6.07 | 65.7 | 2.65 | 3.73 | 6.0 | 21 | FLOW AR @ 97% HUM. |
| M | 0.500 | 17.30 | 6.33 | 65.9 | 2.95 | 3.52 | 65.0 | 21 | FLOW AR @ 100% HUM. |
| N | 0.487 | 14.53 | 5.34 | 67.9 | 2.79 | 2.80 | 1.5 | 21 | FLOW O2 @ 100% HUM. |

B. Nitrogen

CELL NO. 13011

1.1100CM2

| ANNEAL | VOC | JSC | EFF | F.F | G | R | TIME(HR) | TEMP | COMMENTS |
|---|---|---|---|---|---|---|---|---|---|
| A | 0.483 | 16.82 | 6.04 | 66.9 | 3.38 | 2.69 | 20.0 | 150 | FLOW H2 |
| B | 0.494 | 15.44 | 5.79 | 68.4 | 2.38 | 2.83 | 1.5 | 21 | FLOW N2 @ 81% HUM. |
| C | 0.498 | 16.64 | 6.18 | 67.2 | 3.41 | 2.71 | 1.5 | 21 | FLOW N2 @ 88% HUM. |
| D | 0.496 | 16.04 | 5.90 | 66.8 | 4.30 | 2.24 | 1.5 | 21 | FLOW N2 @ 91% HUM. |
| E | 0.493 | 16.64 | 6.10 | 67.0 | 3.21 | 2.90 | 1.5 | 21 | FLOW N2 @ 93% HUM. |
| F | 0.498 | 16.34 | 6.04 | 66.8 | 2.65 | 3.41 | 16.0 | 21 | FLOW N2 @ 97% HUM. |
| G | 0.497 | 18.82 | 6.08 | 65.6 | 4.29 | 2.87 | 8.0 | 21 | FLOW N2 @ 98% HUM. |
| H | 0.496 | 16.40 | 6.02 | 66.6 | 2.84 | 3.33 | 16.0 | 21 | FLOW N2 @ 98% HUM. |
| I | 0.497 | 16.16 | 5.91 | 66.2 | 3.08 | 3.38 | 5.0 | 21 | FLOW N2 @ 99% HUM. |
| J | 0.497 | 16.22 | 5.93 | 66.2 | 3.48 | 3.13 | 16.0 | 21 | FLOW N2 @ 98% HUM. |
| K | 0.498 | 16.34 | 5.97 | 66.0 | 3.43 | 3.27 | 73.5 | 21 | FLOW N2 @ 99% HUM. |
| L | 0.494 | 17.00 | 6.13 | 65.7 | 3.24 | 3.39 | 22.0 | 21 | FLOW N2 @ 100% HUM |
| M | 0.497 | 16.34 | 5.94 | 65.9 | 4.41 | 2.82 | 23.0 | 21 | FLOW N2 @ 100% HUM |
| N | 0.498 | 15.50 | 5.66 | 66.0 | 2.63 | 3.86 | 23.0 | 21 | FLOW N2 @ 100% HUM |
| O | 0.496 | 15.74 | 5.75 | 66.3 | 2.57 | 3.72 | 23.0 | 21 | FLOW N2 @ 100% HUM |
| P | 0.499 | 16.22 | 5.92 | 65.8 | 3.04 | 3.61 | 71.0 | 21 | FLOW N2 @ 100% HUM. |

annealing step may sensitize the cell. It appears that any subsequent exposure of at least 1.5-hrs duration to oxygen or high humidity results in lower $J_{sc}$, although the cell may recover some or all of its current capability later, under aging conditions.

## 3.6 Discussion

We believe that the use of a stress/evaluation tube, which keeps $Cu_2S/CdS$ cells in a continuously controlled ambient during annealing, aging, and evaluation, allows more meaningful assessments to be made of cell performance changes than was possible by previous workers. Even with this improvement, we note that erratic fluctuations in measured performance must be considered carefully before conclusions can be drawn regarding effects of aging in certain gaseous ambients.

Significant degradation of the short-circuit current capability of cells occurs in pure and wet oxygen ambients. In the case of the former, it appears to be limited in time. About 10% loss of $J_{sc}$ occurs within the first 10 hrs for cells aged at room temperature. At 80°C in dry oxygen, the cells we tested lost no more than ~ 20% of their initial $J_{sc}$ capability. There was no evidence for increased losses during aging from 160 to 400 hrs in dry $O_2$ at 80°C.

Cells aged in wet RT ambients exhibit two components of loss, as viewed in terms of time dependence. One component in the loss of $J_{sc}$ is not more than ~ 20% of the initial value. This loss appears to behave exponentially in time, with a time constant of 1 to 3.5 hrs. An additional loss component of $J_{sc}$ is present with a time constant of 35 to 45 hrs. This loss component appears to involve the remainder of initial $J_{sc}$ capability of the cell. Recovery of $J_{sc}$ by annealing in $H_2$ at 150°C is possible, but annealing times of as much as 75 hrs may be required if the current is reduced to <30% of its initial value by aging in wet $O_2$.

If the aging experiments in wet Ar or $N_2$ ambients had resulted in large photocurrent losses (~ 80%) of an exponential character with large time constants (30 to 50 hrs), we might have associated such a loss with the presence of water vapor. Since no such losses occurred experimentally we can only conclude that the large component of $J_{sc}$ loss in wet $O_2$ ambients appears to involve the cooperative action of oxygen and water vapor. As it is, the loss of $J_{sc}$ associated with the shorter time constant for wet $O_2$ may be associated with oxygen sensitivity alone, since a loss in $J_{sc}$ of similar magnitude and time constant was observed for aging in dry $O_2$ at RT and at 80°C.

Palz et al. first suggested that the oxidation of $Cu_2S$ to copper-deficient forms might be the cause of short-circuit current loss in cells exposed to oxidizing ambients.(5) Experimental determinations were made of $J_{sc}$, $V_{oc}$, sheet resistance of the $Cu_2S$, and spectral response for cells with varying degrees of $Cu_2S$ stoichiometry. All samples were prepared identically, then variously anodized, and analyzed by electrochemical methods for stoichiometry. No quantitative justification was given for decreases in short-circuit current in terms of absorption changes.

Peterson and Washburn contended that the reduced absorption of copper-deficient $Cu_xS$ was not sufficient to account for observed reductions in $J_{sc}$. They proposed that dislocation arrays within the $Cu_xS$ layer could attenuate the flux of collected photocarriers by factors of $\sim 0.4$ to 0.8 by providing a very high density of carrier trapping and recombination sites. They have commented that such a model is consistent with the irreversibly deleterious effects on efficiency cells given air exposure at 60°C or higher. In the present work we did not find irreversible degradation for the conditions that were used.

Rothwarf and Windawi have calculated that increases in $\alpha$ by a factor of two can be accounted for by free carrier-absorption effects, without phase change, as the carrier concentration is changed from degenerate ($>10^{20}$ cm$^{-3}$) to nondegenerate ($<10^{19}$ cm$^{-3}$) values.(7) Such a change would produce a 20 to 40% increase in $J_{sc}$ which is observed for cells heated in a reducing atmosphere after aging in air. They also offer a list of eight other mechanisms which were proposed at one time or another to account for experimentally observed changes in $J_{sc}$ in $Cu_2S$/CdS cells. They claim that no convincing quantitative calculations have been made to assess whether particular effects could be significant in actual cells. With regard to the results of the current work, we have observed an effect on $J_{sc}$ which appears to be at least twice as large as that predicted in Ref. 7.

In order to isolate better the physical mechanism for $J_{sc}$ reduction in our experiments, we require direct information on the optical properties of the actual $Cu_2S$ films used in devices. In the next section our efforts at producing test structures to allow such measurements are reviewed.

## 4. OPTICAL CHARACTERIZATIONS OF $Cu_2S$ FILMS IN A CELL CONTEXT

### 4.1 Background

The topological complexity of $Cu_2S$/CdS thin-film cells has made it difficult to characterize the optical behavior of the $Cu_2S$ layer in experimental cells. Such characterization is important since changes in optical properties due to the stoichiometry of the material(8) or to free carrier absorption(7) have been invoked to account for short-circuit current loss as the cells age.(5,7,9) Although techniques exist to characterize the optical absorption of free-standing films of $Cu_2S$, direct measurements in a cell context are more desirable. We have successfully done this for $Cu_2S$ layers of tapered thickness profiles which were formed on single-crystal CdS substrates.* In that case, the planar surfaces of the sample allowed intensity measurements to be made of light passed through the specimen onto a remote silicon detector. These measurements supplied information on the thickness-dependent transmission of light for correlation with local photocurrent response of the $Cu_2S$/CdS device.

In the case of $Cu_2S$ layers in a thin-film cell, measurement with a remote detector introduces additional problems. The roughness of the back surface of the CdS film, after removal of the substrate foil, attenuates the light transmitted out of the sample. In addition, the reproducibility of measurement conditions and results is more difficult than in the single-crystal case. During this quarter we have explored several methods of specimen preparation which would permit fabrication of an integral CdS/$Cu_2S$ detector at the back surface of the CdS film. With such a detector we expected to reduce the optical losses and

---

*Ref. 3, pp. 80-94.

improve the reproducibility of measurements which are associated with the use of remotely situated photodetectors.

### 4.2 Preparation of Integral Detector After Cell Fabrication

We have developed one method for fabricating back-surface detectors which uses previously processed thin-film $Cu_2S/CdS$ cells. After the normal fabrication of such a cell, it is then laminated to a glass plate (with the $Cu_2S$ surface facing the plate). The lamination is done using a method currently employed at Westinghouse for encapsulating arrays of silicon solar cells. A schematic cross-sectional view of the laminated structure is shown in Figure 7. A piece of aluminum foil over the back copper substrate is used to prevent adhesion of the EVA to the copper foil.

To expose the area of interest for back-surface detectors, the back outer layer of aluminum foil and the layers of Teflon©, Korad©, EVA film, and Craneglass© are carefully cut through and then peeled from the laminated workpiece.

Two methods were used to remove an area of the copper substrate and expose the back surface of the CdS film. For one, the copper was etched using $Fe\Psi P_3$ and a painted-on mask of TPA-85 thermoplastic adhesive.* For the other, which was discovered accidentally, the copper foil was peeled from the CdS film. Figure 8 shows a test specimen produced by the etch method.

Conventional cells with gold grids in place were used as the starting point for other test structures. In order to allow comparative measurements of light transmission with and without the presence of a front $Cu_2S$ layer, that layer was removed by etching on about one-half of the cell area. That region is the upper half of the cell area shown in Figure 9a. The light gray, nearly rectangular area in Figure 9a is a

---

*Details on the use of TPA-85 as a mask in front-layer $Cu_2S$ formation are given in Ref. 11, p. 6.

Dwg. 7754A45

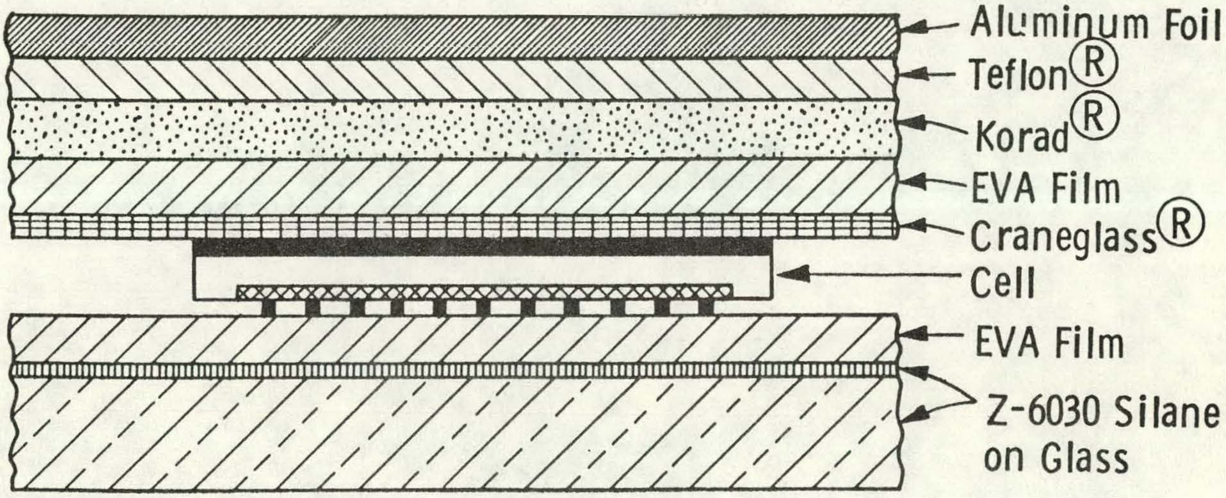

Figure 7. Schematic cross-sectional view of a laminated, encapsulated solar cell.

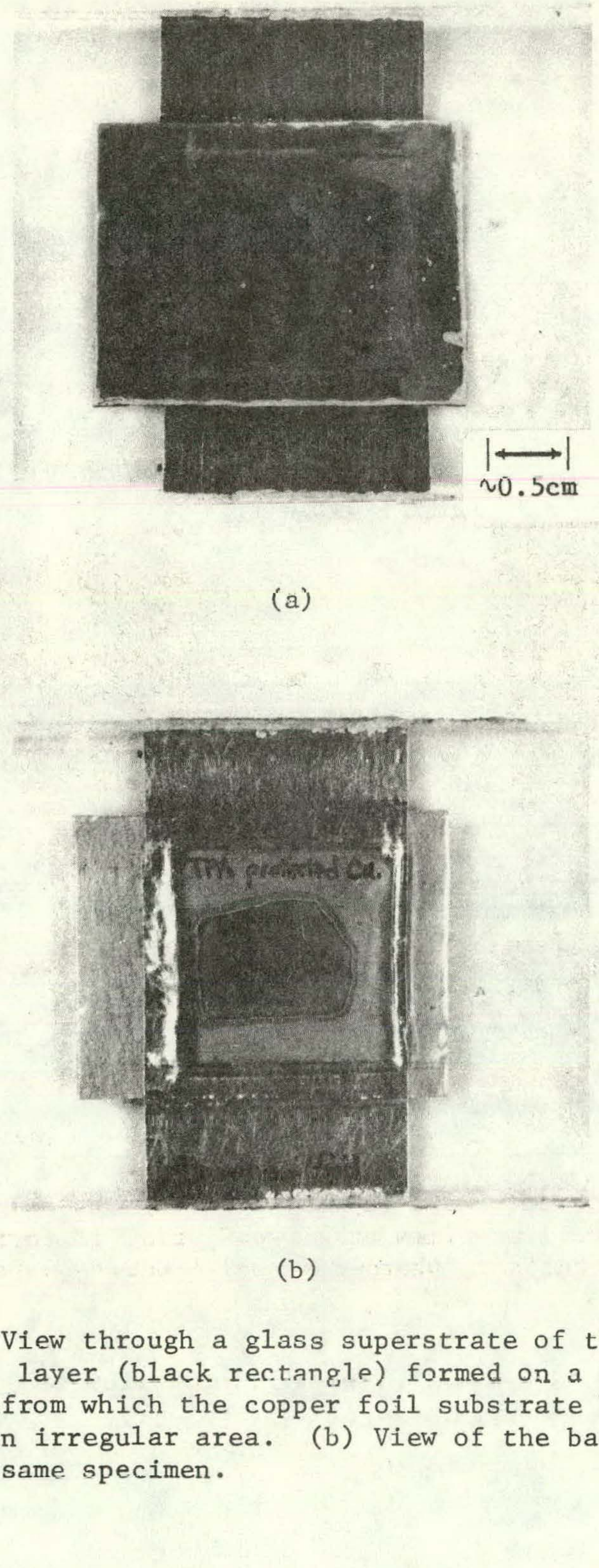

Figure 8. (a) View through a glass superstrate of the top surface $Cu_2S$ layer (black rectangle) formed on a CdS film specimen from which the copper foil substrate has been etched in an irregular area. (b) View of the back surface of the same specimen.

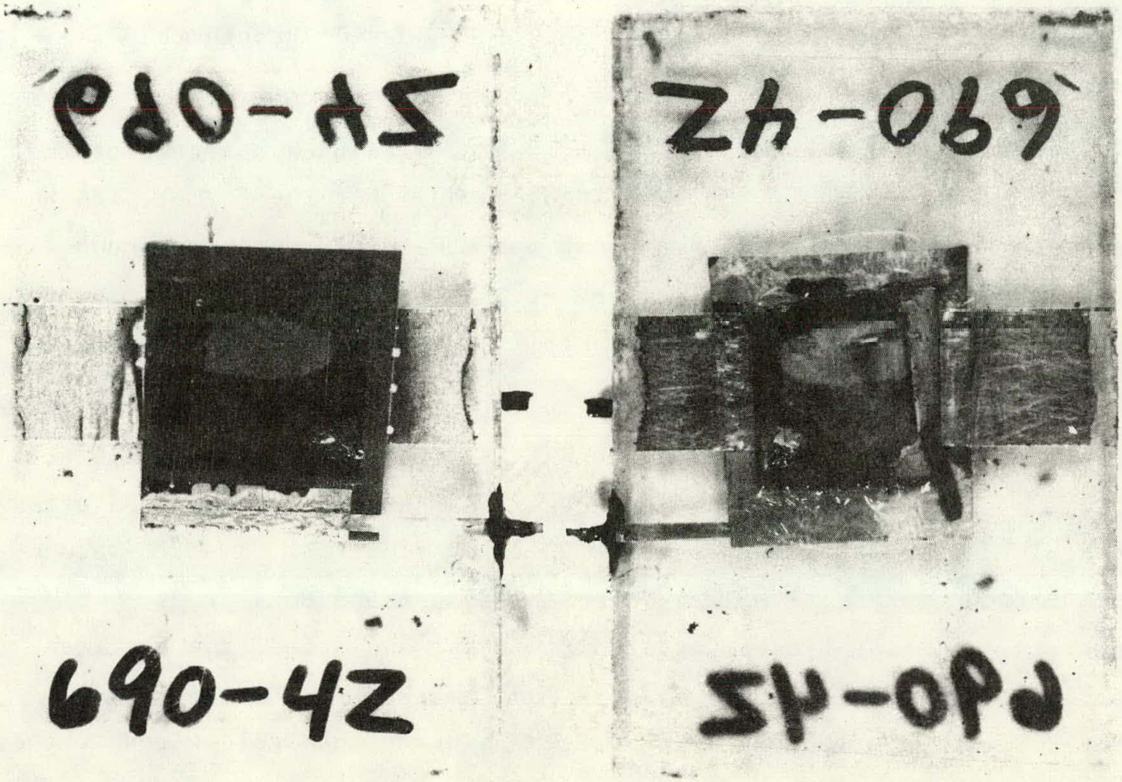

(a) (b)

Figure 9. Views of the front (a) and back (b) surfaces of a solar cell specimen at a stage prior to formation of a back surface, photo-responsive CdS/$Cu_2S$ heterojunction.

portion of the CdS film from which the copper substrate has been removed. Figure 9b shows a view of the back of this specimen with the large, slightly irregular window from which the copper was etched. The area with gridline markings corresponds to the light gray area in Figure 9a. At this stage the specimen is ready for formation of back-surface $Cu_2S$ areas to act as photodetectors for light passed through the specimen from the front.

Local areas of $Cu_2S$ were formed on exposed back surfaces of the CdS films using wet and dry processing methods. For the former, TPA was painted on the surface to mask against the CuCℓ dip except in a number of windows of ~ 0.08 to 0.14 cm diameter. No etching was done prior to the dip in order to minimize the possibility of the $Cu_2S$ from the back surface contacting that from the front.

For dry processing of the back-surface $Cu_2S$, CuCℓ was evaporated through an aperture mask onto the exposed CdS surface to define an array of circular dots, each dot being ~ 0.08 cm in diameter. A short vacuum heat treatment (124°C, 1 hr) rendered the evaporated CuCℓ areas opaque. After being rinsed in deionized water and dried, the specimen was fitted with contacts to the individual back-surface detectors. These contacts were made by using silver paint to bond gold wires to the $Cu_2S$ areas and to aluminum or copper foil tabs which were used for terminal connections. Figure 10 shows a view of the back-surface detectors and contacts on one specimen prepared in this way. The upper four detectors are intended to measure light transmitted through the front-surface $Cu_2S$ layer. The bottom four detectors are in an area from which the front $Cu_2S$ layer has been removed by etching.

The techniques just described were used for fabricating back-surface CdS/$Cu_2S$ heterojunctions as photodetectors on existing $Cu_2S$/CdS thin-film solar cells. Shorting together of the front and back $Cu_2S$ layers was a problem. Electrical measurements between these two layers indicated acceptable isolation only for devices which had been processed in a particular way. That processing involved removal of the copper by

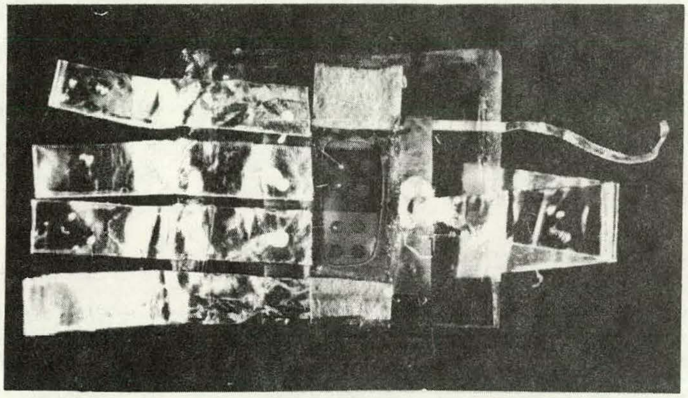

Figure 10. View of the back of a thin film cell specimen with back surface $CdS/Cu_2S$ detectors. Three detectors are wired to foil terminal tabs at the left. At the right, the narrow tab and the wide one are for the front grid and the copper substrate contacts, respectively.

peeling and preparing the back $Cu_2S$ layer by wet processing without any other treatment of that surface. Measurements between the front and back $Cu_2S$ layers indicated back-to-back diode behavior for voltages below 5 to 10V. However, optical measurements with the back-surface detectors which are located under the front $Cu_2S$ layer indicated response from the front $Cu_2S$ layer. Thus, it appears that effective isolation of theee front and back $Cu_2S$ layers is very difficult to achieve. This is probably due to through-the-film paths, such as micro-cracks or other defects, on which $Cu_2S$ may form during processing. Although it may have been possible to solve this problem with additional effort, we elected to try several other more direct methods for implementing the desired measurements.

### 4.3 Preparation of Back-Surface $Cu_2S$ Layers Before Cell Fabrication

We investigated variations of the wet and dry chemistry techniques to prepare $Cu_2S$ layers adjacent to the foil substrate before final fabrication of the front-surface $Cu_2S/CdS$ junction. The wet techniques were not successful due to peeling of the $Cu_2S$ film from the foil substrate. Initially, we tried to form large areas of $Cu_2S$ against bare copper and zinc-plated regions of the foil substrate. This was done by evaporating a thin (1 μm) layer of CdS initially and converting it to $Cu_2S$ by a long (1.25 min) dip in hot $CuC\ell$ solution. At that point some peeling of the film from the substrate was noted. After subsequent deposition of 30 μm of CdS over the $Cu_2S$ layer, the composite layer cracked and flaked from the substrate. There was no difference in adhesion between the zinc-plated and bare copper regions of the substrate. We thought that adhesion might be improved if only small areas of $Cu_2S$ were formed. To test this idea, we deposited the initial thin (1 μm) CdS film through holes of 2 and of 3 mm diameter in a foil mask. After only 20 sec of immersion in hot $CuC\ell$ solution, about half of the 32 $Cu_2S$ areas had flaked from the substrate. We concluded that adherent $Cu_2S$ layers could not be formed in this way for our back-surface detector purposes.

Success was achieved with a back-surface $Cu_2S$ layer formed by first evaporating 8000Å of CuCℓ onto bare copper portions of a foil substrate. A standard CdS film was deposited over the CuCℓ layer. Rectification and photovoltaic behavior were observed on a small sample with an indium dot contact to the CdS film. A 1-$cm^2$ area sample was provided with an evaporated aluminum grid using the standard grid mask. Although the dark reverse-leakage current of the resulting cell was higher than for cells with front-surface $Cu_2S$ layers, the short-circuit current of 800 μA for ~ AM1 illumination indicated adequately high response for use as a back-surface photodetector.

We did not pursue this line of work further. Results of cell-aging experiments suggested that changes in properties of the $Cu_2S$ in cells exposed to mild environment would probably preclude the use of back-surface $CdS/Cu_2S$ detectors. Instead, we began to explore the possibility of preparing CdS films on silicon substrates with the idea of using a monolithic silicon photodetector to measure light transmitted through the overlying thin-film cell structure.

# 5. FUTURE PLANS

Having established that severe degradation of short-circuit current occurs in thin-film $Cu_2S$/CdS solar cells exposed to water vapor/oxygen ambients at room temperature, we will attempt to identify the physical causes for the current loss mechanism. We will continue with work on in-situ measuring of the optical transmission of $Cu_2S$ layers used in thin-film cells. We will also use detailed measurements of photocurrent vs. open-circuit voltage (over a range of illumination levels) for control cells and for those variously aged in wet $O_2$ ambients. This investigation should reveal the extent to which changes in current transport across the heterojunction are involved in the aging process.

# 6. REFERENCES

1. J. R. Szedon, H. C. Dickey, J. A. Abel, and W. J. Biter, "Development of Copper Sulfide/Cadmium Sulfide Thin Film Solar Cells," Sixth Technical Progress Report: 13 October 1980 to 12 January 1981, Contract No. XJ-9-8143-1, July 27, 1981.

2. N. L. Sbar and R. P. Kozakiewicz, 16th Annual Proceedings, Reliability Physics, IEEE Cat. No. 78 CH1 294-8PHY, p. 161 (1978).

3. J. R. Szedon et al., "Cadmium Sulfide/Copper Sulfide Heterojunction Cell Research," Final Report, Contract No. DE-AC03-77ET20429, July 13, 1979.

4. J. R. Szedon, W. J. Biter, J. A. Abel, and H. C. Dickey, Fifth Technical Progress Report, Contract No. XJ-9-8143-1, June 17, 1981.

5. W. Palz, J. Besson, T. Nguyen Duy, and J. Vedel, Conf. Record of the 9th IEEE Photovoltaics Specialists Conf., IEEE Cat. No. 72 CHO 613-0-ED, p. 91 (1972).

6. T. Peterson and J. Washburn, Phys. Stat. Sol.(a), Vol. 22, p. 721 (1974).

7. A Rothwarf and H. Windawi, Conf. Record of the IEEE Photovoltaics Specialists Conf., IEEE Cat. No. 72, p. 722 (1980).

8. B. J. Mulder, Phys. Stat. Sol.(a), Vol. 13, p. 79 (1972).

9. L. C. Burton and H. M. Windawi, J. Appl. Phys., Vol. 47, p. 4621 (October 1976).

## 7. ACKNOWLEDGMENTS

The authors thank G. A. Ferguson, B. A. Blankenship, and H. Shaffer for technical support in preparing CdS films, evaporating the electrodes, and doing photolithography. In particular, the authors thank G. S. Kostyak for his handling of the aging experiments, including the careful acquisition and processing of cell data. They also are grateful to K. B. Haun for preparing the typescript and to G. S. Law for producing the final report.

☆U.S. GOVERNMENT PRINTING OFFICE: 1982-546-085/3012